Clays and Clay Minerals, Vol. 69, No. 1:128–141, 2021

OPTIMIZATION OF HYDROGEN GENERATION BY CATALYTIC HYDROLYSIS OF $NaBH_4$ WITH HALLOYSITE-SUPPORTED COB CATALYST USING RESPONSE SURFACE METHODOLOGY

Seda Hosgun[1,*], Mine Ozdemir[1], and Yeliz Buruk Sahin[2]

[1] Department of Chemical Engineering, Eskişehir Osmangazi University, Eskişehir 26480, Turkey
[2] Department of Industrial Engineering, Eskişehir Osmangazi University, Eskişehir 26480, Turkey

Abstract—The hydrolysis of sodium borohydride ($NaBH_4$) is a promising reaction with a possible practical application as a means of generating hydrogen. The efficiency of hydrogen production can be enhanced significantly by use of a catalyst during the reaction. Cobalt borides show significant catalytic activity, but unsupported CoB particles aggregate easily and are difficult to separate from the reaction medium for re-use. The objectives of the present study were to use halloysite (Hly) as a support material to increase the catalytic activity and reusability of a Co metal-based system and to investigate the binary effect of metal loading and reaction parameters on the hydrolysis of $NaBH_4$. Catalysts were prepared by wet impregnation and chemical reduction. The surface morphology and structural properties of the prepared catalysts were characterized using N_2 adsorption-desorption and the Brunauer-Emmet-Teller (BET) method, field emission scanning electron microscopy (FE-SEM), with energy dispersive X-ray spectroscopy (EDS), X-ray diffraction (XRD), X-ray photoelectron spectroscopy (XPS), and inductively coupled plasma mass spectrometry (ICP-MS). Response surface methodology (RSM) was used to optimize metal loading and reaction conditions for the hydrogen-generation rate. Optimum reaction conditions were determined (using *Design Expert 7.0* software) as 5.01 wt.% Co loading using a Co-B/Hly-supported catalyst, 0.44 M $NaBH_4$, 10.66 mg catalyst, and at a reaction temperature of 39.96°C. The maximum hydrogen generation rate was 33,854 mL min^{-1} $g_{Co}{}^{-1}$ under these conditions.

Keywords—Box Behnken design · CoB · Halloysite · Hydrogen generation · Hydrolysis · $NaBH_4$

INTRODUCTION

Most of the energy used in the world comes from fossil fuels, a major cause of environmental degradation and climate change. This unfavorable situation probably encourages the use of hydrogen as a future energy carrier (Patel & Mitello 2015). Hydrogen has the potential to help meet an increasing global energy demand, including materially promising, economically viable, socially advantageous, and energetically efficient solutions in related fields (Acar & Dincer 2019). Hydrogen-generation technologies have developed in recent decades due to its clean energy properties; high-capacity hydrogen-storage materials have, therefore, attracted much attention. Chemical hydrides contain large amounts of hydrogen and decompose to hydrogen at near room temperature when catalyzed with a suitable catalyst. For this purpose, chemical hydrides such as $NaBH_4$ are very suitable as a source of hydrogen, given their excellent storage properties (Liu et al. 2006). Transition metals (Fe, Co, Ni, and Cu) are used widely in some specific reaction systems due to their low cost, rich reserves, and high activity (Chen et al. 2020). The hydrogen desorption of $NaBH_4$ can be catalyzed successfully using Co-based catalysts. The main disadvantages of using CoO as a catalyst are its poor stability at high temperature and its tendency to agglomerate during reaction (Daza-Gomez et al. 2020).

Catalytic hydrolysis of $NaBH_4$ is a highly complex electrochemical process, but its effectiveness can be increased significantly by using a suitable catalyst. Reaction steps proceed as the borohydride adsorbed on the catalyst surface decomposes, accompanied by the reduction of water with side reactions. Activation of water in the reaction is a limiting step regardless of its excess in the reaction medium (Vinokurov et al. 2018). The hydrolysis reaction with catalysts is as follows:

$$NaBH_4 + 2H_2O \xrightarrow{cat} NaBO_2 + 4H_2 \quad \Delta H = 217 \text{ kJ mol}^{-1} \qquad (1)$$

The hydrolysis of $NaBH_4$ is an exothermic reaction that takes place even at 0°C. Sodium metaborate ($NaBO_2$), which appears as a by-product after the reaction, is an environmentally harmless substance. $NaBO_2$, used as the starting material, provides a possible mechanism to synthesize $NaBH_4$ (Ingersoll et al. 2007; Xu et al. 2007). These obvious advantages in using $NaBH_4$ in hydrogen production make it an attractive method for use in a portable proton exchange membrane (PEM) fuel cell.

Developing heterogeneous catalysts with high activity and durability is important for providing fast and controllable hydrogen production and for easy separation of the catalyst from the reaction medium (Xu et al. 2007). Various catalysts such as those based on ruthenium, platinum, and noble metals have been developed for the hydrolysis reaction of $NaBH_4$. Noble metals-based catalysts show good performance in terms of hydrolysis, but they are not widely available and are expensive; so, the development of alternative,

* E-mail address of corresponding author: serol@ogu.edu.tr
DOI: 10.1007/s42860-021-00113-0

affordable catalysts which are readily available is very desirable. In this context, catalysts such as Ni-B and Co-B show relatively high activity in the hydrolysis reaction. These catalysts are difficult to separate from the reaction medium for reuse, however, due to their powdered nature. In order to solve this problem and to increase the reusability of catalysts, an appropriate support material is needed (Wu et al. 2005; Vinokurov et al. 2018). Various supports such as carbon (Xu et al. 2008), graphene (Li et al. 2014), and clays (Dai et al. 2010) have been used widely to meet this need. The natural abundance and morphological and structural diversity of clay minerals enables their use in many applications in fields ranging from adsorption and water remediation to catalysis and medicine (Krasilin 2020).

Halloysite is a kaolin clay mineral with the formula $Al_2Si_2O_5(OH)_4$; it forms natural aluminosilicate nanotubes. This clay material has tube walls that are 20–30 layers thick, with each layer consisting of one aluminum hydroxide (Al-OH) and one siloxane (Si-O-Si) sheet (a one-to-one ratio), and has multiple inorganic walls (Lim et al. 2020). Rich reagent groups and large surface:volume ratios and a submicron hollow tubular structure allow this material to be used extensively in the synthesis of electronics, catalysis, and industrial materials (Sahiner & Sengel 2017a). Compared to kaolinite, halloysite has a larger specific surface area (Kaze et al. 2020), a property which is of benefit in catalyst-support materials. Halloysite-supported Co_3O_4 for CO oxidation was studied by Daza-Gomez et al. (2020) who found that it was suitable for oxidation of CO thanks to its thermal stability. Various amine functionalized halloysite nanotubes were used by Sahiner and Sengel (2017b) as a catalyst for methanolysis of $NaBH_4$. In that study, a halloysite-supported CoB catalyst was synthesized and used for catalytic hydrolysis to generate hydrogen from $NaBH_4$.

Using response surface methodology (RSM), the effects of various process parameters on the reaction have been studied in detail. The hydrogen-generation reaction with steam methane reforming was analyzed using the Box Behnken Design (Ayodele et al. 2019). *Ethanoligenens harbinense* was used for bio-hydrogen production and Guo et al. (2009) designed an optimum medium using RSM. Work on RSM, including experimental design and regression analysis, by Mishra et al. (2019) led to an optimum substrate-inoculum ratio and initial pH for biological H_2 production from ultrasonic Palm oil mill effluent (POME). The objective of the current study was to investigate the combined effects of reaction conditions on the hydrolysis of $NaBH_4$ and to obtain the maximum hydrogen-generation rate using the smallest amounts of material and energy possible.

EXPERIMENTAL

Materials

Sodium borohydride powder (> 98%) was purchased from Acros Organics (Geel, Belgium); cobalt(II) chloride hexahydrate (> 97%) and sodium hydroxide pellets (> 98%) were supplied by Sigma-Aldrich (Taufkirchen, Germany). Halloysite clay powder (>97%), 30–70 nm × 1–3 μm, with 1.26–1.34 mL/g pore volume was obtained from Sigma-Aldrich (Taufkirchen, Germany).

Catalyst Synthesis

Halloysite was used as the supporting material for the synthesis of Co-B catalysts using the impregnation and reduction method. An appropriate (according to Co loading ratio) amount of $CoCl_2$ solution was prepared with a stoichiometric ratio using distilled water. The Co content in the supported catalysts was adjusted to 5, 10, and 15 wt.%. After impregnation of Co onto halloysite at 75°C for 60 min at 700 rpm, $NaBH_4$ solution was added dropwise to reduce to Co^{2+} any Co that was oxidized during the preparation. Excess borohydride was used in order to provide complete reduction with a molar ratio of $NaBH_4$:$CoCl_2$ of 3:1 and the reduced solution was stirred at room temperature for 60 min at 400 rpm. The sediment was centrifuged (Nuve NF 200, Ankara, Turkey) at 2000 rpm (447 × *g*) for 5 min. Then the sample was collected and washed with an ethanol-water mixture (volume ratio 1:1) in order to remove insoluble, non-clay inorganic material from the catalyst. The sample was placed in the oven at 105°C for 24 h. The powder obtained was black and kept in a dark bottle for use in hydrolysis reactions.

Catalyst Characterization

The morphological structure, crystallinity, and surface composition of the catalysts were characterized by various methods. N_2 sorption isotherms were measured at 77 K using a Tristar 3020 instrument (Micromeritics, Norcross, Georgia, USA). All samples were degassed first at 90°C for 1 h and then at 300°C for 24 h under vacuum before measurement. The specific surface areas of the samples were calculated using the Brunauer-Emmett-Teller (BET) method.

X-ray diffraction (XRD) patterns were obtained using an XRD D8 Advance (Bruker AXS, Karlsruhe, Germany) powder diffractometer. The samples were scanned over the range 20–80°2θ at a scanning rate of 0.5°2θ min^{-1}.

The morphology and surface compositions of the catalysts and halloysite were analyzed using a Regulus 8230 Scanning Electron Microscope (FE-SEM) (Hitachi, Tokyo, Japan) with energy dispersive spectroscopy analysis (EDX).

The Co-based catalysts were dissolved using a microwave-assisted (Milestone, Sorisole, Bergamo, Italy) acid digestion method and analyzed using an inductively coupled plasma mass spectrometer (ICP-MS) (Thermo Scientific iCAP RQ, Waltham, Massachusetts, USA) to determine Co and B.

The surface electronic state was analyzed by X-ray photoelectron spectroscopy (XPS) using a Versaprobe II (PHI5000, ULVAC-PHI, Osaka, Japan) with AlKα (1486.6 eV) as the X-ray source.

https://doi.org/10.1007/s42860-021-00113-0 Published online by Cambridge University Press

The Catalytic Performance of Halloysite-based Catalyst in the Hydrolysis of $NaBH_4$

Hydrogen-production rates from the hydrolysis of $NaBH_4$ were evaluated to determine the catalytic activity of halloysite-supported catalysts. Initially, an appropriate amount of catalyst (10–50 mg) and $NaBH_4$ (0.1–0.5 M) was placed in a 150 mL water-jacketed reactor which maintained the temperature by controlling the circulating water temperature.

The reactor content was mixed using a magnetic stirrer at 400 rpm. During the experiment, the volume of hydrogen generated was recorded using the water-displacement method. Hydrogen-generation rates (HGR, mL min^{-1} g^{-1} catalyst) were calculated from the hydrogen volume as a function of time and the amount of catalyst used.

To determine the optimal reaction conditions of the hydrolysis reaction via $NaBH_4$ using halloysite-supported CoB catalysts, the effects of the amount of catalyst (10–50 mg), $NaBH_4$ initial concentration (0.1–0.50 M), Co loading by weight (5–15%), and temperature (30–50ºC) were studied with a set of values determined by the *Design Expert 7.0* software. The experiments were performed at least twice and the results were given as mean values.

Response Surface Methodology

Response Surface Methodology is defined as: "a set of statistical techniques used to design experiments, build models, evaluate the effects of variables, and determine the optimum conditions of variables to predict a targeted response" (Myers et al. 2016). The Box-Behnken Design (BBD) and Central Composite Design (CCD) are the main techniques of RSM and offer very efficient and cost effective solutions for optimizing complex processes (Jitrwung & Yargeau 2011; Aytar et al. 2014; Hitit et al. 2017; Mishra et al. 2019; Yin & Wang 2019). By enabling consideration of multiple variables and their interactions, they are superior to single-parameter testing approaches. Compared with CCD, the BBD technique does not include extreme-factor value combinations and so, BBD precludes potentially unsatisfactory experimental results (Box & Behnken 1960). In this study, BBD, as an important part of RSM, was utilized to optimize the parameters for hydrogen production.

RESULTS AND DISCUSSION

Characterization of Halloysite-based Co Catalysts

In order to understand the catalytic activity of synthesized catalysts in the hydrolysis of alkaline $NaBH_4$, the textural properties of supports and catalysts were characterized by N_2 sorption measurements. According to IUPAC classification, the adsorption-desorption isotherm characteristics (Fig. 1) conformed to the type IV isotherm (Ayodele et al. 2019). This indicated that the adsorption of the liquid N_2 on the mesoporous Co-B/Hly proceeded via multilayers followed by capillary condensation. An H1-type hysteresis cycle was observed in the range of 0.5–0.95 relative pressure. Pore distribution of catalysts showed that the main pore sizes existed at maximum 14.49, 14.50, 14.50, and 14.64 nm for halloysite, 5Co-B/Hly, 10Co-B/Hly, and 15Co-B/Hly, respectively. This indicated a mesoporous structure for the samples because the main pore sizes were between 2 and 20 nm. The pore characteristics of the halloysite and synthesized catalysts were very similar.

The textural properties of halloysite and synthesized catalysts were characterized by N_2 sorption measurements. The BET specific surface areas of the catalysts were ~87, 77, and 72 m^2/g for 5Co-B/Hly, 10Co-B/Hly, and 15Co-B/Hly, respectively. As expected, the reason the catalyst surface areas are smaller than the surface area of halloysite, 90 mg^2/g, is related to the dispersion of CoB onto/into the support and the increased loading ratio (Table 1). The specific BET surface areas of Co-B/Hly catalysts in this study were greater than those obtained for unsupported Co-B (17 m^2/g) (Yang et al. 2011). The Barrett-Joyner-Halenda adsorption method (BJH) is utilized to define pore area and specific pore volumes through adsorption and desorption techniques (Barrett et al. 1951); the cumulative pore volume of halloysite was 0.205 cm^3/g. The cumulative pore volumes of catalysts for 5Co-B/Hly, 10Co-B/Hly, and 15Co-B/Hly were 0.191, 0.203, and 0.206 cm^3/g, respectively, and the metal loading did not affect significantly the pore volume of the support. The average pore diameter values for halloysite, 5Co-B/Hly, 10Co-B/Hly, and 15Co-B/Hly were 10.95, 11.338, 13.195, and 15.121 nm, respectively. The change in pore diameter with increasing Co load may also be explained by collapse of the support material wall (Hosgun et al. 2020).

The SEM images (Fig. 2) of the halloysite showed the multilayer plate and empty spherical layers. With Co loading, the empty spaces were covered with a slight agglomeration. Condensed structures were found with increasing loading ratio of Co. To determine the chemical composition of the surface of synthesized catalysts, EDS analysis was conducted. From EDS spectra, analysis in three randomly selected regions showed that Co loadings were 7.39, 11.11, and 14.96 wt.% for the 5Co-B/Hly, 10Co-B/Hly, and 15Co-B/Hly catalysts, respectively.

The XRD pattern of halloysite (Fig. 3) showed typical peaks at 11.7, 20.0, 34.9, and 62.3º2θ. The XRD patterns of Co-B/Hly catalysts demonstrated halloysite peaks with intensities varying according to the different loading ratio of catalyst and slight CoO_x peaks (33.0, 37.9, and 42.3º2θ) (Fig. 3) (Vinokurov et al. 2018). The absence of peaks at 44.1°2θ and 51.3º2θ confirmed the precipitation of amorphous Co_2B (Wang et al. 2016).

The ICP-MS analysis was performed to determine the chemical composition of catalysts and the existence of Co and B in the catalysts. The catalyst samples were analyzed after dissolution in nitric acid and pretreatment with microwaves. Cobalt loadings were obtained as 4.8, 9.4, and 14.2 wt.% for the 5Co-B/Hly, 10Co-B/Hly, and 15Co-B/Hly catalysts, respectively (Table 2). The weight percent of B was less than that required to meet stoichiometric needs. Boron loadings were obtained as 1.8, 1.2, and 0.9 wt.% for the 5Co-B/Hly, 10Co-B/Hly, and 15Co-B/Hly catalysts,

https://doi.org/10.1007/s42860-021-00113-0 Published online by Cambridge University Press

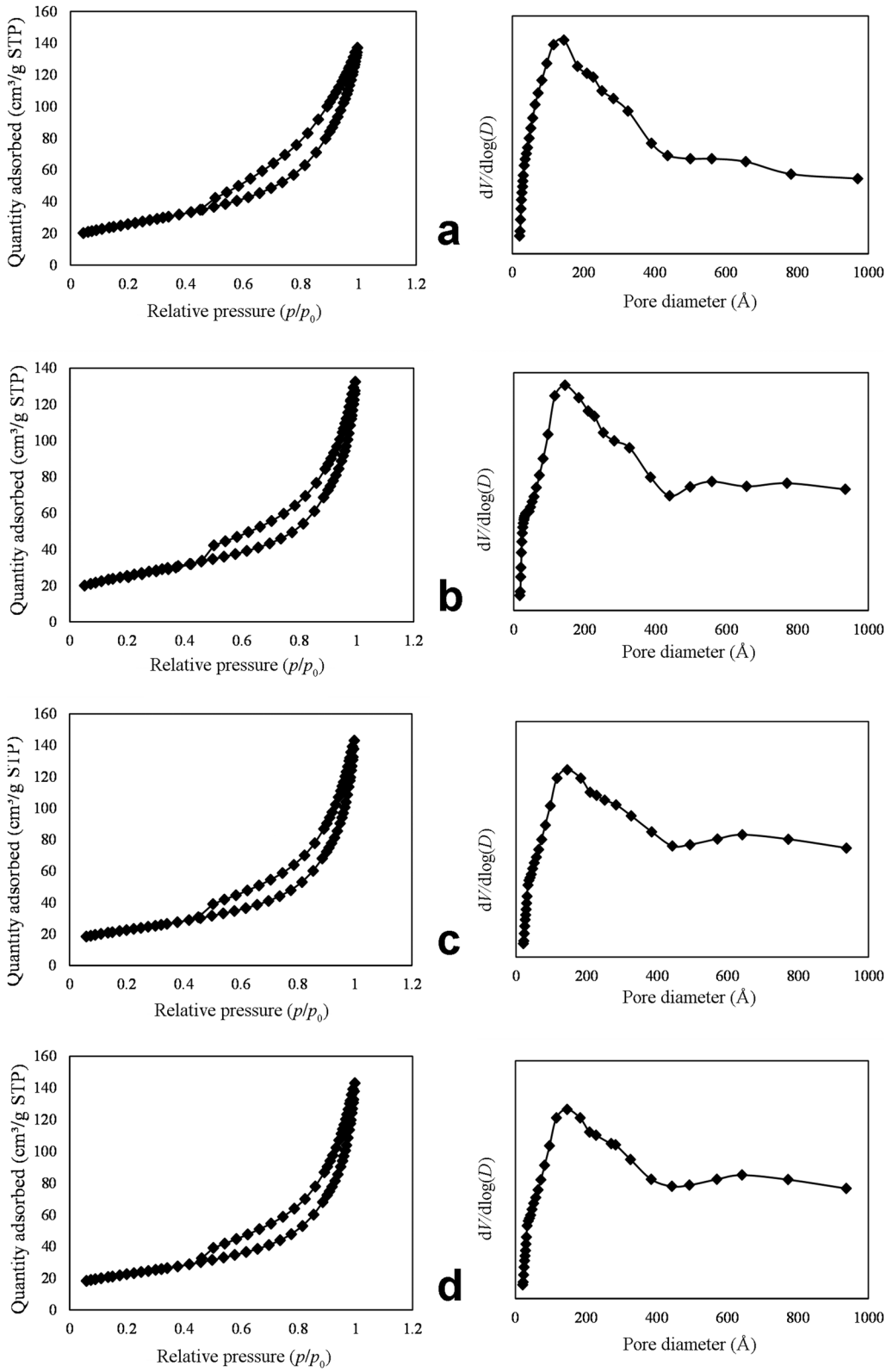

Fig. 1 N_2 adsorption/desorption isotherms and pore distribution of the samples: **a** Halloysite, **b** 5Co-B/Hly, **c** 10Co-B/Hly, and **d** 15Co-B/Hly

https://doi.org/10.1007/s42860-021-00113-0 Published online by Cambridge University Press

respectively. A smaller weight percent of B than the stoichiometrically required amount was also found by Xu et al. (2011), which suggested that the Co metal is adsorbed simultaneously and more easily than B during preparation of the catalyst. The reduction of Co precursors by $NaBH_4$ is a complex process and the product composition depends on the Co:$NaBH_4$ ratio, mixing rate, presence/absence of oxygen, etc. Rapid reaction of the precursors led to the exclusive formation of Co_2B; slower reaction led to side products being formed (Krishnan et al. 2008).

The oxidation states of elements and the surface interaction between atoms in catalysts were analyzed using XPS analysis. The Co_{2p} electron energy levels (Fig. 4a) demonstrated that the Co species in the catalyst samples were present in both elemental and oxidized states, corresponding to binding energies (BE) of ~777.9 eV ($Co_{2p3/2}$) and 794 eV ($Co_{2p1/2}$), respectively (Manna et al. 2014; Wang et al. 2017). The characteristic peak of $Co_{2p3/2}$ for elemental Co of the synthesized catalysts was 777.9 eV. A negative shift of 0.3 eV was observed when the BE of metal Co was compared to the BE of pure Co (778.2 eV). The binding energies of Co for 5Co-B/Hly (793.8 eV), 10Co-B/Hly (794.1 eV), and 15Co-B/Hly (794.3 eV) corresponded to the $Co_{2p1/2}$ peaks of Co^{2+} (Wang et al. 2016).

For B_{1s} XPS peaks (Fig. 4b) at 188.6 eV and 192.5 eV corresponded to the elemental and oxidized B_{1s} levels, respectively. The elemental boron in all the catalyst samples showed a positive shift of 1.5 eV when compared with the BE of pure boron (187.1 eV) (Watts & Wolstenholme 2003; Fernandes et al. 2009). This shift indicated an electron transfer from elemental B to a vacant d-orbital of metallic Co. This created a lack of electrons in elemental boron, while Co metal became enriched with electrons. The presence of high electron density at the catalytically active sites is important for catalytic activity (Fernandes et al. 2009; Wu et al. 2011; Guo et al. 2018).

According to the results above and similar studies (Fernandes et al. 2009; Li et al. 2017), a possible mechanism of the production of H_2 from Co-catalyzed hydrolysis of $NaBH_4$ is proposed that works by following three kinetics steps. In the first step, BH_4^- ions are chemisorbed on the Co atoms; then the hydride ion, H^-, is transferred from BH_4^- ions to adjacent, empty Co atoms. In the last step, this hydrogen atom receives a negative charge in the form of an electron from the Co and leaves the site in hydridic form (H^-) which reacts with the water molecule to produce H_2 and OH^- ions. The OH^- reacts with B in BH_3 to produce $BH_3(OH)^-$ ions. The cycle of hydrogen adsorption on the Co sites lasts until $BH_3(OH)^-$ forms $B(OH)_4^-$. Molecular hydrogen is formed during the full cycle. On the basis of the possible mechanism mentioned, the electron-enriched active Co sites were able to facilitate the catalytic hydrolysis reaction by providing the negative charge electron needed by the hydrogen atom in the last step. As discussed under XPS results, these electrons are supplied by the elemental B to the active Co sites, resulting in Co_2B with high catalytic activity.

Box Behnken Design

In the present study, BBD was applied to determine the effect of four independent variables. The statistical analysis was conducted using *Design Expert 7.0* software. According to BBD, having conducted 27 experiments and collecting the responses, *Y* denotes the generation rate and *A*, *B*, *C*, and *D* represent $NaBH_4$ concentration, catalyst amount, temperature, and metal loading, respectively (Table 3). The factor levels for the hydrogen-generation rate are 0.1, 0.3, and 0.5 M for $NaBH_4$ concentration; 10, 30, and 50 mg for the amount of catalyst; 30, 40, and 50°C for temperature; 5, 10, and 15 wt.% for metal loading.

To determine the effect of synthesized, supported, cobalt-based catalysts on hydrogen generation by $NaBH_4$ hydrolysis, pristine halloysite was tested without any metal loading or modification. The reaction was performed using 50 mg of pristine halloysite, 0.70 M $NaBH_4$, 0.50 g of NaOH at 50°C reaction temperature, and at a 400 rpm stirring rate for the medium, in accord with a previous study (Erol & Özdemir 2017). To compare the halloysite activity, a control experiment was performed under the same reaction conditions without a catalyst. Self-hydrolysis of $NaBH_4$ and hydrolysis using pristine halloysite produced the same amount of H_2 with very close reaction rates. Less than 20 mL of hydrogen generation was seen after 24 h for both studies and conversion of the reaction was not completed. The catalytic activity of pristine halloysite reached a higher reaction rate with any surface modification or any reaction medium optimization.

The most appropriate mathematical models were determined by considering statistical parameters determined by ANOVA and the regression coefficient of the quadratic model was the most appropriate with the Response Surface Reduced Quadratic Model (Table 4).

Table 1 Texture properties of the halloysite and synthesized catalysts

Textural properties	Halloysite	5Co-B/Hly	10Co-B/Hly	15Co-B/Hly
BET surface area (m^2/g)	90.11	87.89	77.712	72.701
Cumulative pore volume (cm^3/g)	0.205	0.191	0.203	0.206
Average pore diameter (nm)	10.95	11.338	13.195	15.121

https://doi.org/10.1007/s42860-021-00113-0 Published online by Cambridge University Press

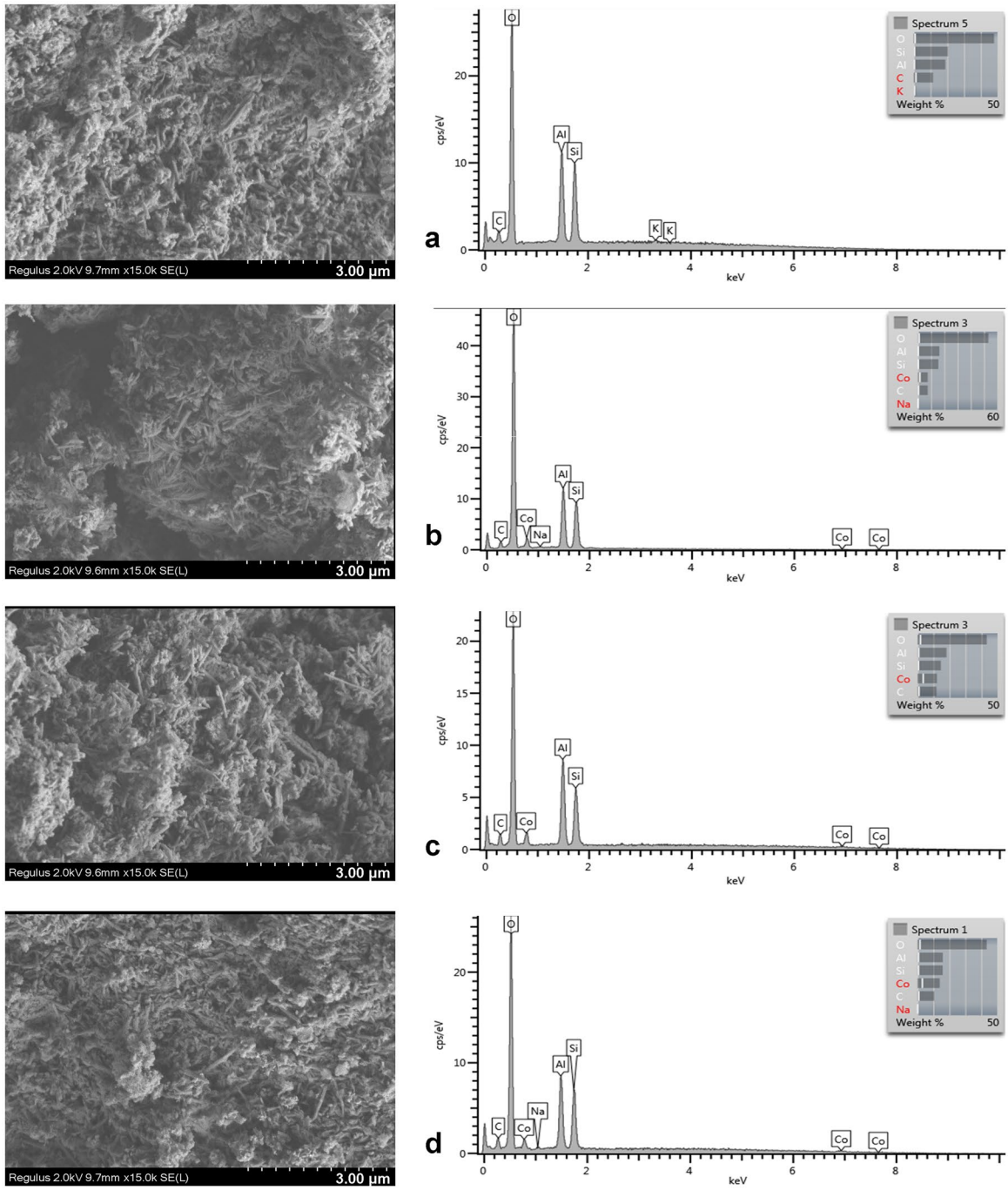

Fig. 2 SEM images and EDX micrographs of: **a** halloysite, **b** 5Co-B/Hly, **c** 10Co-B/Hly, and **d** 15Co-B/Hly

The relationship between variables and responses was determined by the second-order polynomial model. The ANOVA table indicates that the main effects of $NaBH_4$ concentration, catalyst amount, temperature, and metal loading and the second-order effects of catalyst amount×temperature, catalyst amount×metal loading, and metal loading^2 are significant model terms. The reduced quadratic model is presented in Eq. 2:

https://doi.org/10.1007/s42860-021-00113-0 Published online by Cambridge University Press

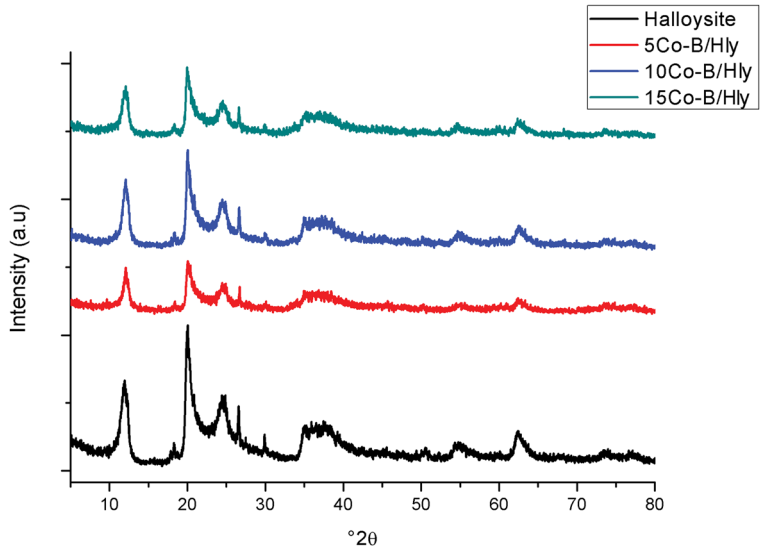

Fig. 3 XRD of CoB halloysite catalysts: 5Co-B/Hly, 10Co-B/Hly, and 15Co-B/Hly

$$\begin{aligned}\mathrm{Log10(Y)} = {} & 3.96 + 0.25 * A - 0.18 * B + 0.12 * C \\ & - 0.11 * D + 0.25 * B * C \\ & - 0.16 * B * D + 0.26D^2\end{aligned} \quad (2)$$

Using *Design Expert 7.0* software, log transformation was found to provide the best fit. The large F value (13.48) and the very low probability ($p < 0.0001$) in ANOVA indicate that the model fits the experimental results adequately (Table 4). The normal probability plot of studentized residuals (Fig. 5) is close to a straight line, which validates the significance of the model (Mishra et al. 2019).

The three-dimensional surface plots represent graphically the regression equations. These plots present the main and interaction effects of two factors, while the other two factors are maintained at fixed levels (Sarac et al. 2017).

The effects of metal loading and amount of catalyst (Fig. 6a) were that the hydrogen-generation rate increased with a decrease in the amount of catalyst from 50 to 10 mg, at a $NaBH_4$ concentration of 0.3 M and temperature of 40°C. The rate of hydrogen generation was calculated using the generated hydrogen volume per reaction total time and catalyst amount. In order to obtain a large hydrogen-generation rate by the hydrolysis reaction, the appropriate amount of catalyst should be used according to the cobalt content of the catalyst. The increase in the amount of catalyst led to an increase in the viscosity of the reaction medium, thereby causing mass transfer limitations. Hydrogen production increased at low metal loading and high $NaBH_4$ concentration (Fig. 6b). With a concentration of 0.3 M $NaBH_4$ and 30 mg of catalyst, when temperature varied from 30 to 50°C and metal loading decreased from 15 to 5 wt.%, the maximum hydrogen-generation rate was obtained (Fig. 6c). The hydrogen-generation rate increased with increasing $NaBH_4$ concentration, but the rate decreased with an increasing amount of catalyst due to mass-transfer limitations (Fig. 6d). The effect of $NaBH_4$ concentration on the hydrogen generation rate was seen more effectively with small amounts of catalyst. Similar studies in the literature show that the hydrogen-generation rate increases to an optimum value, and then decreases (Tian et al. 2010; Li et al. 2017). The reason is that the mass transfer restrictions observed are due to the increase in $NaBO_2$ in the solution phase and also to increased viscosity. The maximum temperature and $NaBH_4$ concentration reveal a maximum hydrogen-generation rate (Fig. 6e). As expected, the reaction rate was faster at high temperatures and showed a linear relationship with reaction time (Sahin et al. 2016). Due to strong binary interactions between catalyst amount and temperature, high temperature increased the hydrogen generation rate with the optimum amount of catalyst (Fig. 6f).

Table 2 Composition of Co-B/Hly catalysts

Samples	Co (wt.%)	B (wt.%)
5Co-B/Hly	4.8	1.8
10Co-B/Hly	9.4	1.2
15Co-B/Hly	14.2	0.9

Determination of Optimal Conditions

The optimal levels of variables and maximum hydrogen production were estimated by desirability function (Ayodele et al. 2019; Derringer & Suich 1980; Wang & Wan 2009). By setting the constraints at predetermined

https://doi.org/10.1007/s42860-021-00113-0 Published online by Cambridge University Press

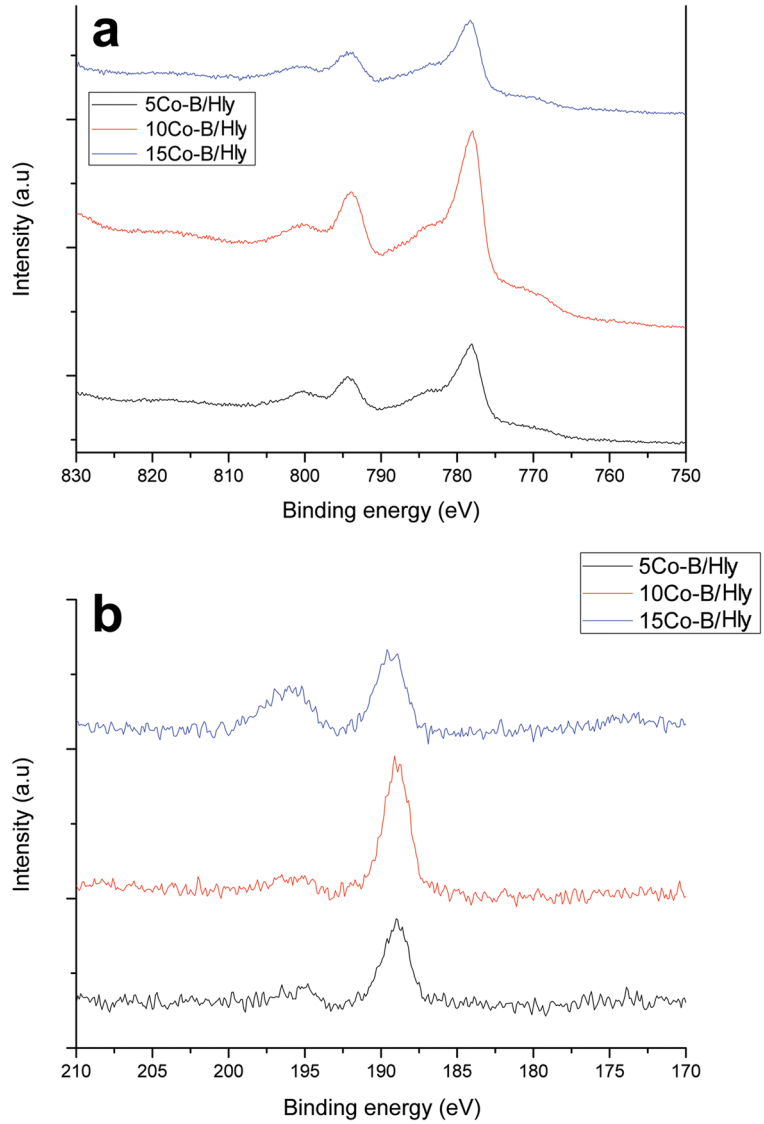

Fig. 4 XPS spectra of: **a** Co_{2p} and **b** B_{1s} level for the Co-B/Hly catalysts

levels, *Design Expert 7.0* software was used to generate a set of solutions ranked according to the desirability values that aimed to maximize hydrogen-generation rate (Table 5).

Ten solutions were obtained with a desirability range from 0.83 to 1.00. Among the solutions, the optimum conditions of 0.44 M, 10.66 mg, 39.96°C, and 5.01 wt.% were selected for $NaBH_4$ concentration, catalyst amount, temperature, and metal loading, respectively. At these levels, the predicted hydrogen production was 33,185.2 mL min^{-1} $g_{Co}{}^{-1}$. To validate the accuracy of the model, an additional, confirmatory experiment was carried out. The objective was to decide whether the conclusions obtained from the analyses were valid. "A useful confirmation is to determine whether the new observation falls within the predicted response interval at that point" according to Montgomery (2017). Three additional experimental runs were employed with the proposed optimal conditions. Repetitive performance tests resulted in hydrogen generation rates of 33,945, 33,873, and 33,744 mL min^{-1} $g_{Co}{}^{-1}$ which were consistent with the RSM optimization. The fact that the results fell into the prediction interval confirmed the validity and adequacy of the predicted models.

A Box Behnken Design was used by Ayodele et al. (2019) to optimize hydrogen production with photocatalytic steam methane reforming in order to investigate the combined effects of irridation time, metal loading, methane concentration, and steam concentration; under optimum conditions, a generation rate of 2.35 μmol H_2/

https://doi.org/10.1007/s42860-021-00113-0 Published online by Cambridge University Press

Table 3 BBD with response of independent variables

Std	Run	*A* (M)	*B* (mg)	*C* (°C)	*D* (%)	Y (mL min^{-1} g_{Co}^{-1})
1	27	0.1	10	40	10	5100
2	11	0.5	10	40	10	16,600
3	25	0.1	50	40	10	4635
4	20	0.5	50	40	10	12,453.7
5	16	0.3	30	30	5	26,215
6	17	0.3	30	50	5	32,422.5
7	14	0.3	30	30	15	16,529
8	5	0.3	30	50	15	14,300
9	3	0.1	30	40	5	5788
10	23	0.5	30	40	5	30,200.4
11	7	0.1	30	40	15	5300.2
12	15	0.5	30	40	15	22,744.3
13	10	0.3	10	30	10	20,245
14	21	0.3	50	30	10	2358.9
15	6	0.3	10	50	10	10,985.4
16	12	0.3	50	50	10	12,750
17	24	0.1	30	30	10	3753.4
18	9	0.5	30	30	10	8271.8
19	13	0.1	30	50	10	10,526
20	19	0.5	30	50	10	25,252
21	26	0.3	10	40	5	32,451
22	22	0.3	50	40	5	19,673.2
23	2	0.3	10	40	15	32,575
24	4	0.3	50	40	15	4569.6
25	8	0.3	30	40	10	10,850
26	1	0.3	30	40	10	10,680
27	18	0.3	30	40	10	8550

min was obtained with 3 wt.% La/TiO_2. The effects of reaction conditions on sodium borohydride-to-hydrogen generation using the Box-Wilson optimization technique was studied by Ozkan et al. (2019). Optimization of the catalyst loading for the direct borohydride fuel cell (DBFC) was studied by San et al. (2016) with the power density of the fuel cell chosen as a response (dependent) parameter. Catalyst loading is an important factor for DBFC performance. Increasing the catalyst loading was expected to increase fuel cell performance, but increasing the amount of catalyst more than was required affected the power density of the fuel cell adversely. This was because the active centers of the catalyst particles became clogged with increasing viscosity. CoB/SiO_2 was used by Yang et al. (2011) to catalyze the hydrolysis reaction of $NaBH_4$. Those authors found that a SiO_2-supported CoB catalyst showed activity which was four times greater than unsupported CoB catalysts with a rate of 10,586 mL min^{-1} g^{-1} at 298 K. A hydrogen generation rate of 2400 mL min^{-1} g^{-1} was recorded by Jeong et al. (2007) using a CoB catalyst calcined at 250ºC.

Optimization of a hydrolysis reaction for hydrogen generation using Co-based metal oxide nanocrystals was studied by Kim et al. (2020), who reported a maximum hydrogen-production rate of 10,367 mL min^{-1} g^{-1} at 293 K via $NaBH_4$ hydrolysis with wüsite cobalt oxide nanorods (wz-CoO-NRs). In a study by Zhang et al. (2019), a maximum rate of 5955 mL min^{-1} g^{-1} hydrogen at 298 K was achieved by $NaBH_4$ hydrolysis using a non-noble Co-based nanoporous graphene oxide catalyst. A 8333 mL min^{-1} g^{-1} rate of H_2 generation at 303 K using CoO nanorods was found by Lu et al. (2012). A maximum H_2 generation rate (303 K) of 6130 mL min^{-1} g^{-1} was reported by Zhang et al. (2015) for porous CoO nanorods (length of >500 nm). A maximum hydrogen generation rate of 2218 mL min^{-1} g^{-1} with methanolysis of sodium borohydride using various halloysite-supported

https://doi.org/10.1007/s42860-021-00113-0 Published online by Cambridge University Press

Table 4 ANOVA for Response Surface Reduced Quadratic Model

Source	Sum of Squares	Degrees of Freedom	Mean Square	F-value	p-value Prob > F	
Model	2.23	7	0.32	13.48	< 0.0001	significant
A	0.76	1	0.76	32	< 0.0001	
B	0.37	1	0.37	15.61	0.0009	
C	0.17	1	0.17	7.19	0.0148	
D	0.15	1	0.15	6.41	0.0203	
BC	0.25	1	0.25	10.52	0.0043	
BD	0.1	1	0.1	4.27	0.0526	
D^2	0.43	1	0.43	18.35	0.0004	
Residual	0.45	19	0.024			
Lack of Fit	0.44	17	0.026	7.79	0.1197	not significant
Pure Error	0.007	2	0.003			
Cor Total	0.68	26				

R-squared: 0.8324; Adj R-squared: 0.7706

functionalized amine groups was achieved by Sahiner and Sengel (2017b). An 18,700 mL min^{-1} $g_{Co}{}^{-1}$ hydrogen-production rate with 16 wt.% of a Co-loaded halloysite catalyst was obtained by Vinokurov et al. (2018) using several preparation techniques which included wet impregnation and surface modification of halloysite with ligand assistance. In the present study, however, using a chemical reduction method in addition to wet impregnation to allow better distribution of metal, higher catalytic activity enabled the authors to obtain a hydrogen-generation rate of 33,854 mL min^{-1} $g_{Co}{}^{-1}$ using 5.01 wt.% Co metal loading.

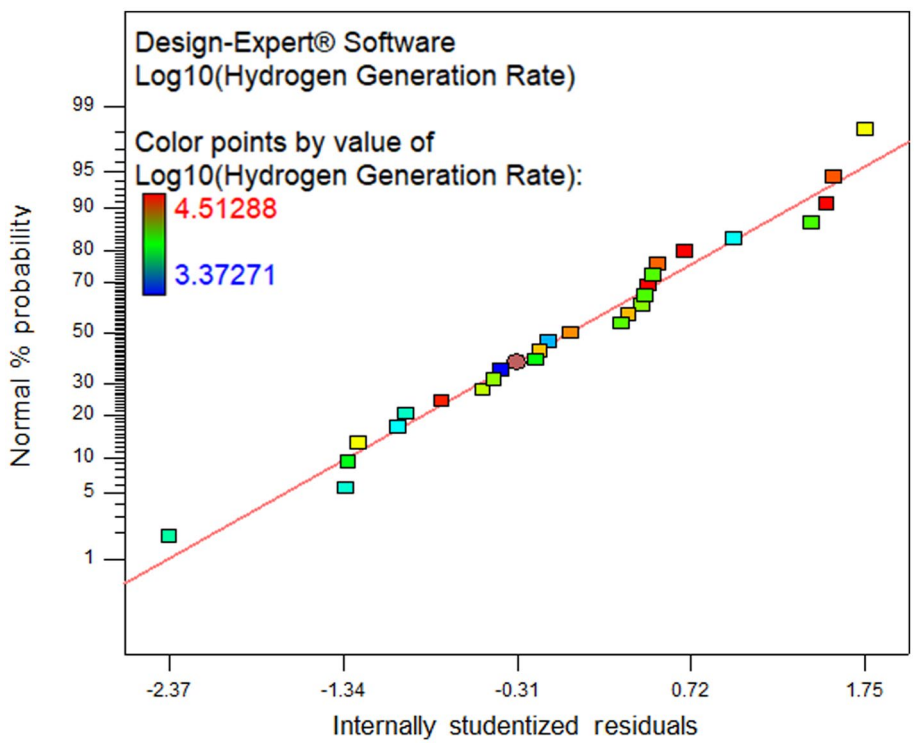

Fig. 5 Normal probability versus internally studentized residuals for the hydrogen generation rate

https://doi.org/10.1007/s42860-021-00113-0 Published online by Cambridge University Press

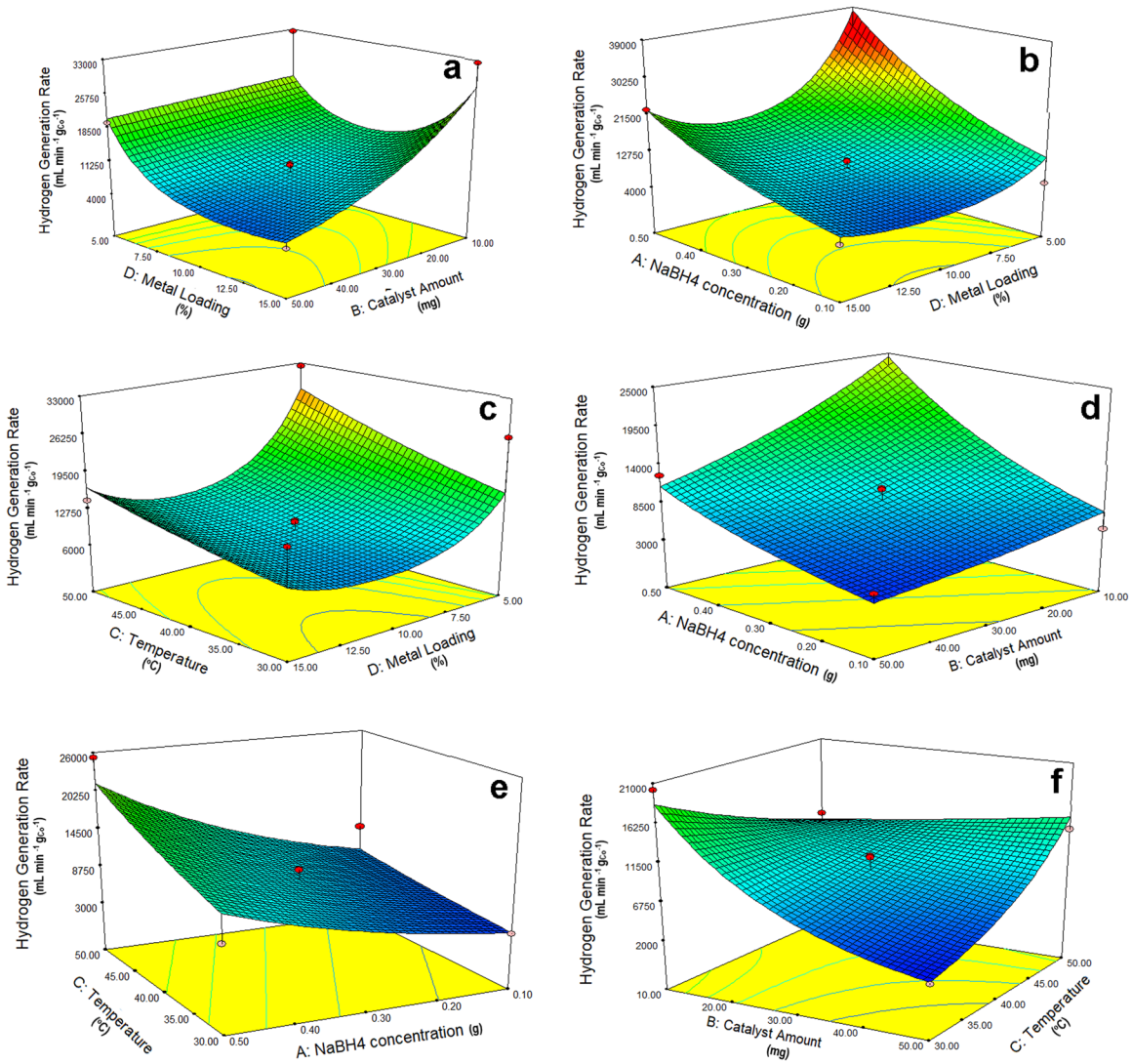

Fig. 6 Response surface curves for hydrogen-generation rate

Table 5 Optimum conditions based on desirability

Number	*A* (M)	*B* (mg)	*C* (°C)	*D* (%)	*Y* (mL $min^{-1}g_{Co}^{-1}$)	Desirability	Decision
1	0.44	10.66	39.96	5.01	33185.2	1	selected
2	0.36	41.86	46.18	5.32	32755.2	1	
3	0.5	19.83	48.89	14.99	32959	1	
4	0.31	10.72	31.96	14.8	32773.8	1	
5	0.5	19.33	47.97	14.9	32619.9	1	
6	0.46	21.01	36.76	5.2	32663.1	1	
7	0.48	18.4	45.46	15	32407.8	1	
8	0.12	49.76	50	5	28359.9	0.953	
9	0.5	50	36.74	5.01	27698.5	0.938	
10	0.31	10	49.63	15	21177.8	0.834	

https://doi.org/10.1007/s42860-021-00113-0 Published online by Cambridge University Press

CONCLUSION

Halloysite-supported Co-B catalysts were synthesized using impregnation and chemical reduction methods for sodium borohydride hydrolysis. Halloysite was used as a support material because of its thermal stability and physicochemical and microstructural properties. The individual and interactive effects of $NaBH_4$ concentration, catalyst amount, temperature, and metal loading on hydrogen generation were investigated using BBD. A set of optimal points for hydrogen generation was determined by the desirability function. ANOVA results showed that significant interaction effects occurred between the amount of catalyst and the temperature, and also between the amount of catalyst and the metal loading. Those showed that the hydrolysis reaction was affected significantly by the amount of Co in the catalyst. The concentration of the $NaBH_4$ solution also affected the hydrolysis reaction profoundly and the rate of reaction was greater with a higher reactant concentration, correlated with the amount of BH_4^-. The reason for the lower reaction rate at a greater concentration than the optimum value was the formation of a blocking layer on the catalyst surface consisting of sodium metaborate. A maximum hydrogen generation rate of 33,854 mL min^{-1} g_{Co}^{-1} was obtained at an $NaBH_4$ concentration of 0.44 M, catalyst amount of 10.66 mg, temperature of 39.96°C, and metal loading of 5.01 wt.%. The selected conditions used less material, consumed less energy, and prevented the mass-transfer restriction for the catalytic hydrolysis medium due to low viscosity. The results suggested that statistical design methodology offers an efficient and feasible approach for optimization of the hydrogen-generation medium; and halloysite-supported CoB is a suitable catalyst for catalytic hydrolysis of $NaBH_4$ with significant hydrogen generation.

Declarations

Conflict of Interest

The authors declare that they have no conflict of interest.

REFERENCES

Acar, C., & Dincer, I. (2019). Review and evaluation of hydrogen production options for better environment. *Journal of Cleaner Production, 218,* 835–849.

Ayodele, B. V., Ghazali, A. A., Yassin, M. Y. M., & Abdullah, S. (2019). Optimization of hydrogen production by photocatalytic steam methane reforming over lanthanum modified Titanium (IV) oxide using response surface methodology. *International Journal of Hydrogen Energy, 44*(37), 20700–20710.

Aytar, P., Gedikli, S., Buruk, Y., Cabuk, A., & Burnak, N. (2014). Lead and nickel biosorption with a fungal biomass isolated from metal mine drainage: Box-Behnken experimental design. *International Journal of Environmental Science and Technology, 11*(6), 1631–1640.

Box, G. E., & Behnken, D. W. (1960). Some new three level designs for the study of quantitative variables. *Technometrics, 2*(4), 455–475.

Chen, D., Liu, C., Mao, Y., Wang, W., & Li, T. (2020). Efficient hydrogen production from ethanol steam reforming over layer-controlled graphene-encapsulated Ni catalysts. *Journal of Cleaner Production, 252,* 119907.

Dai, H. B., Kang, X. D., & Wang, P. (2010). Ruthenium nanoparticles immobilized in montmorillonite used as catalyst for methanolysis of ammonia borane. *International Journal of Hydrogen Energy, 35*(19), 10317–10323.

Daza-Gomez, L. C., Ruiz-Ruiz, V. F., Mendoza-Nieto, J. A., Pfeiffer, H., & Diaz, D. (2020). Co_3O_4 nanostructures and Co_3O_4 supported on halloysite nanotubes: New highly active and thermally stable feasible catalysts for CO oxidation. *Applied Clay Science, 190,* 105590.

Derringer, G., & Suich, R. (1980). Simultaneous optimization of several response variables. *Journal of Quality Technology, 12,* 214–219.

Elliott, E. P., Barrett, E. P., Joyner, L. G., & Halenda, P. P. (1951). The determination of pore volume and area distributions in porous substances. I. Computations from nitrogen isotherms. *Journal of the American Chemical Society, 73*(1), 373–380.

Erol, S., & Özdemir, M. (2017). Development of Co-B/Magnesite catalyst for hydrogen generation by Hydrolysis of sodium borohydride. *Journal of The Turkish Chemical Society: Section B Engineering, 1,* 69–76.

Fernandes, R., Patel, N., Miotello, A., & Filippi, M. (2009). Studies on catalytic behavior of Co-Ni-B in hydrogen production by hydrolysis of $NaBH_4$. *Journal of Molecular Catalysis A: Chemical, 298,* 1–6.

Guo, W. Q., Ren, N. Q., Wang, X. J., Xiang, W. S., Ding, J., You, Y., & Liu, B. F. (2009). Optimization of culture conditions for hydrogen production by EthanoligenensharbinenseB49 using response surface methodology. *Bioresource Technology, 100*(3), 1192–1196.

Guo, J., Hou, Y., Li, B., & Liu, Y. (2018). Novel Ni-Co-B hollow nanospheres promote hydrogen generation from the hydrolysis of sodium borohydride. *International Journal of Hydrogen Energy, 43,* 15245–15254.

Hitit, Z. Y., Lazaro, C. Z., & Hallenbeck, P. C. (2017). Hydrogen production by co-cultures of Clostridium butyricum and Rhodospeudomonas palustris: Optimization of yield using response surface methodology. *International Journal of Hydrogen Energy, 42*(10), 6578–6589.

Hosgun, H. L., Ture, A. G., Hosgun, E. Z., & Bozan, B. (2020). Synthesis 5-hydroxymethylfurfural (5-HMF) from fructose over cetyl trimethylammonium bromide-directed mesoporous alumina catalyst: effect of cetyl trimethylammonium bromide amount and calcination temperature. *Reaction Kinetics, Mechanisms and Catalysis, 129,* 337–347.

Ingersoll, J. C., Mani, N., Thenmozhiyal, J. C., & Muthaiah, A. (2007). Catalytic hydrolysis of sodium borohydride by a novel nickel–cobalt–boride catalyst. *Journal of Power Sources, 173*(1), 450–457.

Jeong, S. U., Cho, E. A., Nam, S. W., Oh, I. H., Jung, U. H., & Kim, S. H. (2007). Effect of preparation method on Co-B catalytic activity for hydrogen generation from alkali $NaBH_4$ solution. *International Journal of Hydrogen Energy, 32,* 1749–1754.

https://doi.org/10.1007/s42860-021-00113-0 Published online by Cambridge University Press

Jitrwung, R., & Yargeau, V. (2011). Optimization of media composition for the production of biohydrogen from waste glycerol. *International Journal of Hydrogen Energy, 36*(16), 9602–9611.

Kaze, C. R., Alomayri, T., Hasan, A., Tome, S., Lecomte-Nana, G. L., Nemaleu, J. G. D., Tchakoute, H. K., Kamseu, E., Melo, U. C., & Rhaier, H. (2020). Reaction kinetics and rhelogical behaviour of meta-halloysite based geopolymer cured at room temperature: Effect of thermal activation on physiochemical and microstructural properties. *Applied Clay Science, 196,* 105773.

Kim, C., Lee, S. S., Li, W., & Fortner, J. D. (2020). Towards optimizing cobalt based metal oxide nanocrystals for hydrogen generation via $NaBH_4$ hydrolysis. *Applied Catalysis A: General, 589,* 117303.

Krasilin, A. A. (2020). Energy modeling of competition between tubular and platy morphologies of chrysotile and halloysite layers. *Clays and Clay Minerals, 68,* 436–445.

Krishnan, P., Advani, S. G., & Prasad, A. K. (2008). Cobalt oxides as Co_2B catalyst precursors for the hydrolysis of sodium borohydride solutions to generate hydrogen for PEM fuel cells. *International Journal of Hydrogen Energy, 33*(23), 7095–7102.

Li, X., Fan, G., & Zeng, C. (2014). Synthesis of ruthenium nanoparticles deposited on graphene-like transition metal carbide as an effective catalyst for the hydrolysis of sodium borohydride. *International Journal of Hydrogen Energy, 39*(27), 14927–14934.

Li, Z., Wang, L., Zhang, Y., & Xie, G. (2017). Properties of Cu-Co-P/γ-Al_2O_3 catalysts for efficient hydrogen generation by hydrolysis of alkaline $NaBH_4$ solution. *International Journal of Hydrogen Energy, 42,* 5749–5757.

Lim, S., Park, S., & Sohn, D. (2020). Modification of halloysite nanotubes for enhancement of gas-adsorption capacity. *Clays and Clay Minerals, 68,* 189–196.

Liu, B. H., Li, Z. P., & Suda, S. (2006). Nickel- and cobalt-based catalysts for hydrogen generation by hydrolysis of borohydride. *Journal of Alloys and Compounds, 415,* 288–293.

Lu, A., Chen, Y., Jin, J., Yue, G. H., & Peng, D. L. (2012). CoO nanocrystals as a highly active catalyst for the generation of hydrogen from hydrolysis of sodium borohydride. *Journal of Power Sources, 220,* 391–398.

Manna, J., Ror, B., Vasthistha, M., & Sharma, P. (2014). Effect of Co^{+2}/BH_4^- ratio in the synthesis of Co-B catalysys on sodium borohydride hydrolysis. *International Journal of Hydrogen Energy, 39,* 406–413.

Mishra, P., Ameen, F., Zaid, R. M., Singh, L., Ab Wahid, Z., Islam, M. A., & Al Nadhari, S. (2019). Relative effectiveness of substrate-inoculum ratio and initial pH on hydrogen production from palm oil mill effluent: Kinetics and statistical optimization. *Journal of Cleaner Production, 228,* 276–283.

Montgomery, D. C. (2017). *Design and analysis of experiments.* John Wiley and Sons.

Myers, R.H., Montgomery, D.C., & Anderson-Cook, C.M. (2016). *Response Surface Methodology: Process and Product Optimization using Designed Experiments.* John Wiley & Sons, Hoboken, New Jersey, USA.

Ozkan, G., Akkus, M. S., & Ozkan, G. (2019). The effects of operating conditions on hydrogen production from sodium borohydride using Box-Wilson optimization technique. *International Journal of Hydrogen Energy, 44*(20), 9811–9816.

Patel, N., & Mitello, A. (2015). Progress in Co–B related catalyst for hydrogen production by hydrolysis of boron-hydrides: A review and the perspectives to substitute noble metals. *International Journal of Hydrogen Energy, 40*(3), 1429–1464.

San, F. G. B., Karadag, C. I., Okur, O., & Okumus, E. (2016). Optimization of the catalyst loading for the direct borohydride fuel cell. *Energy, 114,* 214–224.

Sarac, N., Uğur, A., Simsek, Ö., Aytar, P., Toptas, Y., Buruk, Y., Cabuk, A., & Burnak, N. (2017). Phenol Tolerance and Biodegradation Optimization of Serratia Marcescens NS09-1 Using Plackett-Burman and Box-Behnken Design. *Environmental Engineering and Management Journal, 16*(11), 2637–2645.

Sahin, Ö., Kılınc, D., & Saka, C. (2016). Bimetallic Co-Ni based complex catalyst for hydrogen production by catalytic hydrolysis of sodium borohydride with an alternative approach. *Journal of Energy Institute, 89,* 617–626.

Sahiner, N., & Sengel, S. (2017). Environmentally benign halloysite clay nanotubes as alternative catalyst to metal nanoparticles in H_2 production from methanolysis of sodium borohydride. *Fuel Processing Technology, 158,* 1–8.

Sahiner, N., & Sengel, S. (2017). Various amine functionalized halloysite nanotube as efficient metal free catalyst for H_2 generation from sodium borohydride methanolysis. *Applied Clay Science, 146,* 517–525.

Tian, H., Guo, Q., & Xu, D. (2010). Hydrogen generation from catalytic hydrolysis of alkaline sodium borohydride solution using attapulgite clay-supported Co-B catalyst. *Journal of Power Sources, 195,* 2136–2142.

Vinokurov, V., Sitavitskaya, A., Gulatov, A., Ostudin, A., Sosna, M., Gushchin, P., Darrat, Y., & Lvov, Y. (2018). Halloysite nanotube-based cobalt mesocatalysts for hydrogen production from sodium borohydride. *Journal of Solid State Chemistry, 268,* 182–189.

Wang, J., & Wan, W. (2009). Application of desirability function based on neural network for optimizing bio hydrogen production process. *International Journal of Hydrogen Energy, 34*(3), 1253–1259.

Wang, Y., Li, T., Bai, S., Qi, K., Cao, Z., Zhang, K., Wu, S., & Wang, D. (2016). Catalytic hydrolysis of sodium borohydride via nanostructured cobalt–boron catalysts. *International Journal of Hydrogen Energy, 41*(1), 276–284.

Wang, L., Li, Z., Zhang, Y., Zhang, T., & Xie, G. (2017). Hydrogen generation from alkaline $NaBH_4$ solution using electroless-deposited Co-Ni-W-P/γ-Al_2O_3 as catalysts. *Journal of Alloys and Compounds, 702,* 649–658.

Watts, C. F., & Wolstenholme, J. (2003). *An Introduction to Surface Analysis by XPS and AES.* Wiley-Blackwell, Oxford, UK.

Wu, C., Bai, Y., Liu, D. X., Wu, F., Pang, M. L., & Yi, B. L. (2011) Ni–Co–B catalyst-promoted hydrogen generation by hydrolyzing NaBH4 solution for in situ hydrogen supply of portable fuel cells. *Catalysis Today, 170*(1), 33–39.

Wu, C., Wu, F., Bai, Y., Yi, B., & Zhang, H. (2005). Cobalt boride catalysts for hydrogen generation from alkaline $NaBH_4$ solution. *Materials Letter, 33,* 7385–7391.

Xu, D., Zhang, H., & Ye, W. (2007). Hydrogen generation from hydrolysis of alkaline sodium borohydride solution using Pt/C catalyst. *Catalysis Communications, 8*(11), 1767–1771.

Xu, D., Dai, P., Liu, X., Cao, C., & Guo, Q. (2008). Carbon-supported cobalt catalyst for hydrogen generation from alkaline sodium borohydride solution. *Journal of Power Sources, 182*(2), 616–620.

Xu, D., Wang, H., Guo, Q., & Ji, S. (2011). Catalytic behavior of carbon supported Ni-Bi Co-B and Co-Ni-B in hydrogen

generation by hydrolysis of KBH_4. *Fuel Processing Technology, 92,* 1606–1610.

Yang, C. C., Chen, M. S., & Chen, Y. W. (2011). Hydrogen generation by hydrolysis of sodium borohydride on CoB/SiO_2 catalyst. *International Journal of Hydrogen Energy, 36*(2), 1418–1423.

Yin, Y., & Wang, J. (2019). Optimization of fermentative hydrogen production by Enterococcus faecium INET2 using response surface methodology. *International Journal of Hydrogen Energy, 44*(3), 1483–1491.

Zhang, H., Ling, T., & Du, X. W. (2015). Gas-Phase cation exchange toward porous single-crystal CoO nanorods for catalytic hydrogen production. *Chemistry of Materials, 27*(1), 352–357.

Zhang, H., Feng, X., Cheng, L., Hou, X., Li, Y., & Han, S. (2019). Non-noble Co-anchored on nanoporous graphene oxide, as an efficient and long-life catalyst for hydrogen generation from sodium borohydride. *Colids and Surfaces A: Physicochemical and Engineering Aspect, 563,* 112–119.

(Received 26 September 2020; revised 26 January 2021; AE: Hongping He)